Computers and Structures xxx (2016) xxx–xxx

Contents lists available at ScienceDirect

Computers and Structures

journal homepage: www.elsevier.com/locate/compstruc

Effects of specimen size on assessment of shrinkage cracking of concrete via elliptical rings: Thin vs. thick

Wei Dong [a], Xiangming Zhou [b,*], Zhimin Wu [a], Gediminas Kastiukas [b]

[a] State Key Laboratory of Coastal and Offshore Engineering, Dalian University of Technology, Dalian 116024, PR China
[b] Department of Mechanical, Aerospace and Civil Engineering, Brunel University, London UB8 3PH, UK

ARTICLE INFO

Article history:
Accepted 16 December 2015
Available online xxxx

Keywords:
Early-age concrete
Crack initiation
Cracking propagation
Geometry effect
Fracture mechanics
Restrained shrinkage

ABSTRACT

An elliptical ring test method is proposed to replace the circular ring test recommended by ASTM and AASHTO for faster and more reliable assessment of cracking tendency of concrete. Numerical models are also established to simulate stress development and crack initiation/propagation in restrained concrete rings. Cracking age, position and propagation in various rings are obtained from numerical analyses that agree well with experimental results. Elliptical thin rings of certain geometry can shorten the ring test duration as desirable. In thin rings, crack initiation is caused by external restraint effect so that a crack occurs at the inner circumference and propagates towards the outer one. In thick rings, crack initiation is mainly due to the self-restraint effect so that a crack occurs at the outer circumference and propagates towards their inner one. Therefore, thick elliptical concrete rings do not necessarily crack earlier than circular ones as observed from experiment.

1. Introduction

Shrinkage cracking of concrete occurs when the tensile stress generated due to restrained volume contraction of concrete exceeds its tensile strength. Shrinkage cracking is a major problem for flat concrete elements/structures with a large exposed surface area-to-volume (A/V) ratio, such as industrial floors, concrete pavements and bridge decks. The cracking of concrete can reduce its load carrying capacity and accelerate deterioration, increasing maintenance costs and shortening the service life of concrete structures. So far, several test methods have been developed to assess how susceptible a given concrete mixture may be to cracking. ASTM C 341 [1] adopts 400 mm long and 100 mm square concrete prisms, with all surfaces exposed for drying, to assess free shrinkage of concrete by monitoring their longitudinal length change. Although free shrinkage measurement is helpful in comparing different mix proportions, they do not provide sufficient information to determine how concrete will crack in service [2]. Rather, the cracking tendency of concrete has been mainly evaluated under restrained conditions by qualitative means through a range of tests, such as the bar, the plate/slab and the ring tests. Among these, the circular ring test has been widely used for assessing cracking tendency of concrete and other cement-based materials due to its simplicity and versatility [3–4].

As a standard test method, the circular ring test was first approved by the American Association of State Highway and Transportation (AASHTO). The standard AASHTO PP34-99: Standard Practice for Estimating the Cracking Tendency of Concrete is used for the determination of the cracking tendency of restrained concrete specimens.

This consists of a concrete ring with an inner diameter of 305 mm, a wall thickness and height of 75 and 150 mm, respectively. The concrete ring surrounds a restraining steel ring with an outer diameter of 305 mm and a wall thickness of 12.5 mm. A 75 mm thick concrete ring is called a thick ring in this study. ASTM also follows by recommending the circular ring test (ASTM C1581/C1581M-09a: Standard Test Method for Determining Age at Cracking and Induced Tensile Stress Characteristics of Mortar and Concrete under Restrained Shrinkage). Different from AASHTO, ASTM recommends thin rings with a reduced wall thickness of 37.5 mm to initiate cracking at an earlier age and to shorten the duration of the ring test. Casting a concrete ring around a steel core, usually a steel ring is the basic principle of the circular ring test. This restrains the concrete shrinkage, resulting in tensile stress developing in the concrete ring and compressive stress in the steel core. If the tensile stress exceeds the critical material limit of concrete, cracks will initiate. It has been found that the cracking age depends not only on the properties of concrete but also on the degree of restraint provided by the central restraining steel core in the ring test. Detection of the first cracking may result in a long waiting period due to either the restraining core not being stiff

* Corresponding author.
E-mail address: Xiangming.Zhou@brunel.ac.uk (X. Zhou).

http://dx.doi.org/10.1016/j.compstruc.2015.12.005
0045-7949/

enough or the concrete being characterised with high cracking resistance. Sometimes a visible crack may not even be generated in concrete rings [5,6]. Although AASHTO and ASTM recommended standard dimensions of circular ring specimens, other circular ring geometries [3,4,6–10] have been used in various studies. Alternatively, novel elliptical ring geometries were adopted to replace circular ring geometries [11–14]. Although not proven in studies [11–14], cracks initiating earlier in elliptical ring rather than in circular ones due to stress concentrations caused by geometrical effects is the generally accepted theory. Besides, in contrast with the fact that a crack may initiate anywhere in a circular ring specimen, for an elliptical ring specimen of a given geometry, it tends to be at a determinable position, reducing the resources needed for detecting crack initiation/propagation in the ring test. Therefore, elliptical ring specimens have been employed for assessing cracking tendency of cement-based materials as an improved ring test by some researchers [11–16]. However, most of those studies focused on investigating the effects of variations in material proportions/additives on the restrained shrinkage cracking of concrete or other cement-based materials.

The mechanism of the elliptical ring test has been largely unexplored since only Zhou et al. [15] and Dong et al. [16] have conducted research trying to figure out under which conditions the elliptical ring cracks earlier than circular ones. However, those studies only focused on thin rings. No study has been carried out on investigating the mechanism of the thick ring test. It should be noted that ASTM thin rings are not appropriate for concrete with large aggregates whereas the AASHTO thick rings are. In addition, no comparison test has been conducted using thick circular and elliptical rings, so there is no scientific evidence available to indicate whether thick elliptical rings crack earlier than thick circular ones. Furthermore, the geometrical effect of the central restraining ring on initial cracking age of a thick concrete ring is not reported in literature. Therefore, it is significant to quantify the impact of ring geometry including ring wall thickness on the degree of restraint to concrete surrounding it in the ring test.

Many studies have been carried out so far on analysing cracking of concrete in restrained circular ring specimens. In a circular concrete ring specimen, the restraining effect from the central steel ring on the surrounding concrete ring can be conveniently replaced by a pressurising force applied to the interface between the steel and concrete rings in numerical analyses [3,6,17–19]. In comparison, very limited analytical/numerical research has been carried out on elliptical concrete rings under restrained shrinkage. He et al. [11] assumed that an elliptical concrete ring is subject to a uniform internal pressure provided by the central steel core. This is the same assumption taken in analysing shrinkage cracking in circular ring specimens by many other researchers [3,6,17–19].

In fact, due to geometrical effect, the radial deformation of the central restraining elliptical steel ring is not uniform along its circumference when concrete shrinks [15,16]. Therefore, it is believed that the uniform internal pressure assumption is not appropriate for elliptical ring specimens. Meanwhile, the degree of restraint is largely dependent on the geometry of the central restraining steel ring. Especially important is its major and minor semi-axes which are believed to have a significant effect on the initial cracking age and cracking position of a concrete ring surrounding it.

Moreover, it is believed that the thickness of a concrete ring wall has a significant effect on stress development in concrete under restrained shrinkage. AASHTO PP34-99 recommends thick rings with a concrete wall thickness of around 75 mm while ASTM C1581/C1581M-09a recommends thin rings with a wall thickness of around 37.5 mm. Therefore it is necessary to investigate how a concrete mixture may exhibit different cracking behaviours in thick and thin rings respectively. Experiments have indicated that thicker concrete sections exhibited higher resistance to cracking than thinner ones, suggesting that the age of concrete cracking is different in structures with different thickness [20]. Due to the increase in wall thickness, a complex stress field occurs across the wall of a concrete ring specimen when drying from its outer circumferential cylindrical surface. Unlike for thin rings, the analysis of thick rings using the assumption of uniform stress across a concrete ring is considered inappropriate. Besides, experiments have indicated that a crack initiates at the outer circumference and propagates towards to the inner one in thick rings when drying from their outer circumferential surface [21]. Alternatively, a crack would initiate at the inner circumference of a thick ring and propagate towards the outer one if based on the assumption of uniform strain across the ring wall. In order to characterise stress development while considering the effect of ring geometry and drying direction, analytical models were developed to assess residual stress in restrained ring specimens [4,6,7,20,21]. However, it should be noted that those analytical models were developed for circular rings only and may not be appropriate for elliptical ones.

In line with this, a numerical approach is developed to simulate the behaviour of concrete in restrained ring specimens. Fictitious temperature fields are applied on a concrete ring specimen to simulate the mechanical effect of concrete shrinkage on the ring under a restrained condition. The fictitious temperature fields are derived based on free shrinkage tests of concrete prisms. When the exposed drying surface area-to-volume ratio of a concrete ring specimen is equal to that of a concrete prism in a free shrinkage test, both specimens can be regarded as being under the same temperature field. To obtain the internal stress in the concrete, the fictitious temperature field is used to generate thermal loading on the restrained concrete rings through combined thermal and structural analyses. Moreover, the stress intensity factor can be obtained by fracture analysis. Cracking age, position and propagation in a series of circular and elliptical, both thin and thick concrete ring specimens subject to restrained shrinkage are analysed using the numerical model established in this study. Besides, experiments have also been conducted on those concrete rings under restrained shrinkage conditions. To verify the numerical analysis approach, its results are compared with the initial cracking ages of those rings. Finally, the effects of ring geometry on cracking age, position and propagation in concrete rings under restrained shrinkage are also discussed to explore further the mechanism of the ring test. From this, it is aimed to propose practical guidance in choosing appropriate ring geometry for assessing cracking tendency of concrete and other cement-based materials. By extending the Zhou et al. conference paper [22], a deeper investigation is made and includes the following additional research:

(1) The numerical analysis adopts a nonlinear distribution of moisture loss, hence drying shrinkage, across a thick concrete ring wall. In comparison, a linear distribution of moisture loss, across a thick concrete ring wall was employed in the numerical model established in the conference paper. It is regarded that a nonlinear distribution of moisture loss is more appropriate for a thick concrete ring wall [4,6].
(2) A fracture mechanics-based analysis model and concrete cracking criterion are adopted in this paper for analysing thick concrete rings subject to restrained shrinkage. While in the conference paper, an elastic analysis was employed on thick concrete rings with the maximal tensile stress cracking criteria for concrete. A fracture mechanics-based analysis model and concrete cracking criterion are regarded to be more appropriate for analysing thick concrete rings [2,10,16].
(3) A deeper analyses on the restraining effect on thick concrete rings has been conducted in this paper, in which the restraining effects are separated into the following two

Please cite this article in press as: Dong W et al. Effects of specimen size on assessment of shrinkage cracking of concrete via elliptical rings: Thin vs. thick. Comput Struct (2016), http://dx.doi.org/10.1016/j.compstruc.2015.12.005

parts: (a) circumferential self-restraint due to nonlinear moisture loss and therefore nonlinear drying restraint across a thick concrete ring wall; (b) external restraining effect along the radial direction from the central restraining steel ring. The corresponding tensile stress/stress intensity factor due to these two types of restraining effects has been obtained through numerical analyses. It has been found that during crack propagation, the self-restraining effect remains almost constant however the external restraining effect increases with the propagation of crack. The self-restraining effect dominates in the regions near the exposed outer circumferential surface, driving crack propagation. As a crack propagates close to the inner circumferential surface of a concrete ring, the combined restraining effects from the self-restraint and external restraint dominate. These results, which are totally new and reveal the mechanism of the elliptical ring test, did not appear in the conference paper.

(4) From the numerical analyses in this study, it has been found that once a crack starts to propagate in a thick concrete ring, it will continuously propagate throughout the ring wall very quickly. Therefore in the numerical analyses, the age at which a crack starts to propagate is actually the age of cracking of a thick concrete ring. The driving force for crack initiation and propagation in a thick concrete ring is the self-restraining effect due to nonlinear circumferential drying rather than the external restraint effect from the central steel ring. This is the reason why elliptical thick rings do not crack earlier than the circular ones. If any sealing condition allows the moisture distribution, and therefore shrinkage, across the ring wall to become uniform, then the self-restraint effect from concrete itself will be largely reduced. In this case, the restraining effect to a thick concrete ring will mainly come from the central steel ring, i.e. external restraint and is revealed for the first time in this paper. By such modification, the thick ring test recommended by AASHTO will better serve its purpose.

It is expected that the experimental and numerical investigations presented here will lead to a better understanding on how the elliptical ring geometry affects stress development and crack initiation/propagation in restrained concrete rings. Additionally, the proposed elliptical ring test can complement the circular ring tests recommended by ASTM and AASHTO for faster and more reliable assessment of the likelihood of cracking of concrete and other cement-based materials. Also the elliptical ring test can be conveniently employed for assessing the effects of variations in the proportions and material properties of mortar or concrete on cracking tendency. These may include aggregate source, gradation, aggregate-cement paste bond, cement type and content, water content, mineral/chemical admixtures, fibre reinforcement, etc. The elliptical ring test can also be adopted for evaluating factors that may affect concrete cracking such as curing time, curing method, and evaporation rate.

2. Experimental

In this study, two series of circular and elliptical concrete ring specimens were subject to circumferential drying under restrained shrinkage to investigate the initial cracking age, position and crack propagation in concrete rings. Concrete wall thicknesses of 37.5 and 75 mm referred to as "thin rings" and "thick rings", respectively, were made. The shapes and notations of the circular and elliptical ring geometries tested in this study are shown in Fig. 1. The concrete mix proportions for making those specimens was 1:1.5:1.5:0.5 (cement: sand: coarse aggregate: water) by weight with the maximal coarse aggregate size of 10 mm, representing a normal weight and normal strength concrete.

2.1. Thin ring test

Thin ring tests were performed conforming to ASTM C1581/C1581M-09a. Five different ring geometries, with the inner major radius a always equalling 150 mm but the inner minor radius b varying from 150, 125, 100, 75 to 60 mm were tested. Two rings for each of the five different ring geometries were subjected to restrained shrinkage under the drying environment of 23 °C and 50% RH. The wall thickness, t, of the restraining steel rings and concrete rings was 12.5 and 37.5 mm, respectively. The height of the rings was kept constant at 75 mm. Four strain gauges were attached, each at one equidistant mid-height, on the inner circumferential surface of the central restraining steel ring. These were connected to a data acquisition system in a half-bridge configuration that can automatically record the circumferential strain of the inner surface of the restraining steel ring continuously. Following the ASTM C1581/C1581M-09a protocol, the top and bottom surfaces of the concrete rings were sealed using two layers of aluminium tape and drying was only allowed from their outer circumferential cylindrical surface. The instrumented ring specimens were finally moved into an environmental chamber for drying until cracks occurred. The instrumented ring specimens, data acquisition system and the environment chamber for drying concrete specimens are shown in Fig. 2. In order to eliminate the effect of friction between concrete and steel, the outer circumferential surface of the steel ring in contact with the inner circumferential surface of the concrete ring, was coated with a release agent as suggested by AASHTO PP34-99 and ASTM C1581/C1581M-09a.

In the restrained ring test, the inner steel ring restrains the shrinkage of the maturing concrete. Therefore, tensile stress develops in the concrete ring along its circumferential direction and accordingly compression stress in the restraining steel ring. The increase in compression stress in the steel ring with age is reflected

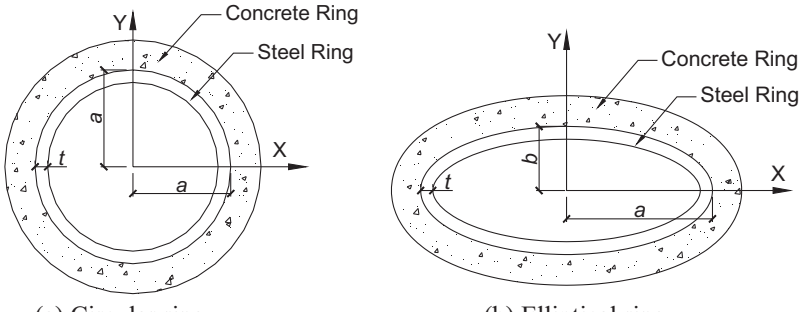

(a) Circular ring (b) Elliptical ring

Fig. 1. Notations of geometries of ring specimens.

Please cite this article in press as: Dong W et al. Effects of specimen size on assessment of shrinkage cracking of concrete via elliptical rings: Thin vs. thick. Comput Struct (2016), http://dx.doi.org/10.1016/j.compstruc.2015.12.005

(a) Sealed ring specimens

(b) Environmental chamber and strain gauge data acquisition system

(c) Ring specimens in chamber

Fig. 2. Instrumented ring test set-up.

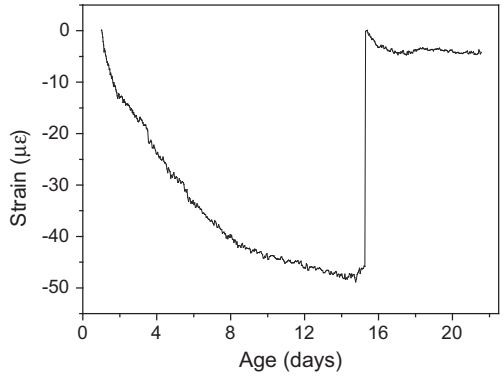

Fig. 3. Recorded strain with age in a restraining steel ring from experiment.

by the increase in the strain recorded by the strain gauges attached on the inner surface of the steel ring. When the maximum circumferential tensile stress developed in the concrete ring exceeds the tensile strength of concrete, cracks will initiate. The tensile stress close to the crack in the concrete ring is then released resulting in a sudden drop in compression stress in the steel ring. This is reflected by a sudden drop in strain recorded by the strain gauges. Based on this, the age of crack initiation is determined, which is the same technique adopted by ASTM C1581/C1581M-09a and AASHTO PP34-99 for cracking detection. Fig. 3 provides a graphical representation of the strain recorded from the elliptical ring using the data acquisition system.

Cracking ages of a series of circular and elliptical thin rings, subject to restrained shrinkage, observed from experiment results are listed in Table 1. It can be seen that the elliptical rings with a geometrical factor $a/b < 2$, i.e. those with $a = 150$ mm, and $b = 125$, or 100 mm, did not crack earlier than the circular ones with

Table 1
Average cracking ages (in days) obtained from numerical analyses and experiment.

$a \times b$ mm^2	Concrete ring wall thickness					
	37.5 mm			75 mm		
	Num.	Exp.		Num.	Exp.	
150 × 150	18	15	14	16	–	–
125 × 125	–	–	–	18	19	25
150 × 125	20	15	14	17	20	21
150 × 100	17	15	14	18	21	22
150 × 75	11	10	10	21	18	18
150 × 60	12	11	15	–	21	19

$a = 150$ mm. This suggests that these elliptical ring geometries do not provide the expected higher degree of restraint compared to the circular ones. This indicates that the initial cracking ages of these circular and elliptical ring specimens are very close to the values of around 15 days. However, the elliptical ring specimens with $a/b \geqslant 2$, i.e. those with $a = 150$ mm, and $b = 75$ or 60 mm, cracked earlier than the circular ones, in this case at 10 days on average for the former and at 13 days on average for the latter, respectively. Therefore, from experimental results, it can be concluded that elliptical ring specimens with a/b between 2 and 3, crack earlier in ring tests due to an enhanced degree of restraint and thus higher development of concrete tensile stresses.

2.2. Thick ring test

Thick ring specimens with a 75 mm thick wall, as recommended by AASHTO PP34-99, were also tested under restrained shrinkage conditions. Two rings for each of the five different ring geometries were prepared as listed in Table 1. Following the same procedures as for the thin rings, the specimens were dried under the environment of 23 °C and 50% RH, under restrained conditions

Please cite this article in press as: Dong W et al. Effects of specimen size on assessment of shrinkage cracking of concrete via elliptical rings: Thin vs. thick. Comput Struct (2016), http://dx.doi.org/10.1016/j.compstruc.2015.12.005

until at least one crack propagated throughout the ring wall. Top and bottom surfaces of the rings were sealed with the outer circumferential surface exposed to drying. The experimental procedure adopted for the thick rings was the same as that for thin rings described in Section 2.1. It should be noted that no circular thick ring with $a = 150$ mm was tested due to the size restriction of the environment chamber. A circular thick ring specimen with $a = 125$ mm was tested instead. Cracking ages of the thick rings from experiments are listed in Table 1. The circular thick ring specimens with $a = 125$ mm cracked at an age of 22 days. Elliptical ring specimens with an increasing geometrical factor a/b i.e. minor semi-axis b decreasing from 125, 100, 75 to 60 mm achieved cracking ages of 21, 22, 18, and 20 days, respectively, as observed from experimental results. It seems that the impact of the elliptical shape on shortening cracking age in thick rings is not as significant as that in thin ones.

3. Numerical

Since experimental results suggested that circular and elliptical steel rings to the surrounding concrete provide different degrees of restraint, it is significant to investigate stress development in restrained concrete rings. Therefore, a numerical approach was developed to explore the mechanism of the circular and elliptical ring tests. In this numerical approach, finite element analyses were carried out using ANSYS code to simulate stress/stress intensity factor with age in a concrete ring specimens, under restrained shrinkage until cracking initiated. It should be noted that the ANSYS code does not directly support shrinkage loading neither does it allow a direct entry for shrinkage as a material property because unlike concrete, most engineering materials do not undergo shrinkage. Therefore, as an alternative method, a fictitious temperature field applied on concrete ring specimens in the numerical analyses represented the shrinkage effect of concrete.

3.1. Fictitious temperature field

The volumetric change of concrete can usually be classified into two broad categories: thermal shrinkage and drying shrinkage [20,21]. Thermal shrinkage of concrete is a result of cement hydration and/or changes in environmental temperature while drying shrinkage is the response of concrete to moisture movement. There is an obvious difference between thermal and drying shrinkage with the latter largely dependent on the A/V ratio of a concrete element. When a concrete element is subjected to a drying environment without any restraint, its size/volume will change. This phenomenon is often referred to as free shrinkage and as a result does not cause any stress in concrete. In this study, firstly the free shrinkage of concrete was measured using prismatic specimens with different A/V ratios to simulate different exposure conditions, by monitoring their longitudinal length change. The length change for concrete prisms experiencing free shrinkage can be regarded to be the same as when exposed to a fictitious temperature field. As a result, the relationship between free shrinkage and fictitious temperature field can be established for concrete at various ages through numerical analyses. In line with this, concrete prisms with the dimensions of 285 mm in length and 75 mm square in cross section, conforming to ISO 1920-8, were subjected to drying without any restraint in the same environment as for curing concrete ring specimens. Their longitudinal length change was monitored by a dial gauge, which was then converted into shrinkage strain. Considering that concrete shrinkage depends on a concrete element's A/V ratio, the following four different exposure conditions each with an individual A/V ratio, were investigated: all surfaces sealed ($A/V = 0$), all surfaces exposed for drying ($A/V = 0.060$/mm), two side surfaces with the dimensions of 285×75 mm^2 exposed for drying ($A/V = 0.027$/mm) and one side surface exposed for drying ($A/V = 0.013$), (see Fig. 4). Double-layer aluminium tape was used to seal the surfaces that were not intended for drying. Fig. 5 shows the measured average free shrinkage strain of concrete at various ages up to 28 days under the four exposure conditions.

Another assumption adopted in the numerical analyses is that free shrinkage is the same for concrete elements with the same A/V ratio but of different geometry/shape. In this case, there will be an identical fictitious temperature field applied to concrete specimens with the same A/V ratio but of different geometry/shape resulting in a volume change matching that of the concrete prisms. This assumption can also be applied to a concrete ring specimen in a restrained shrinkage test in the numerical analyses. In summary, the fictitious temperature drop-age relationship for a concrete ring specimen can be established based on the free shrinkage-age relationship of concrete prisms obtained from free shrinkage tests. The fictitious temperature field acting on the concrete ring specimen makes it shrink.

3.1.1. Thin ring specimens

In the case of a thin ring, concrete shrinkage can be regarded to be uniform across its wall. The relationship between the fictitious temperature drop and its corresponding A/V ratio for thin concrete elements, regardless of their geometry/shape and at various ages can be obtained by introducing a linear thermal expansion coefficient of concrete, 10×10^{-6}/°C in this case, as presented in Fig. 6. Although Fig. 6 only presents the curves at 3-day intervals, the temperature drop was actually calculated for each day using the above method that was then used to update the input data for the finite element analyses. Meanwhile, as an example, Fig. 7

Fig. 4. Sealed concrete prisms mounted for free shrinkage test.

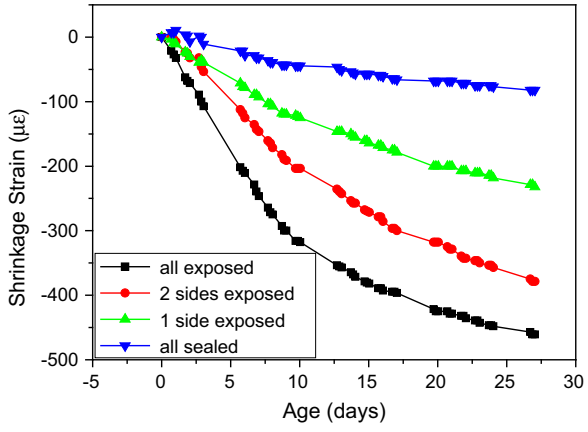

Fig. 5. Shrinkage strain of concrete obtained from free shrinkage test.

Please cite this article in press as: Dong W et al. Effects of specimen size on assessment of shrinkage cracking of concrete via elliptical rings: Thin vs. thick. Comput Struct (2016), http://dx.doi.org/10.1016/j.compstruc.2015.12.005

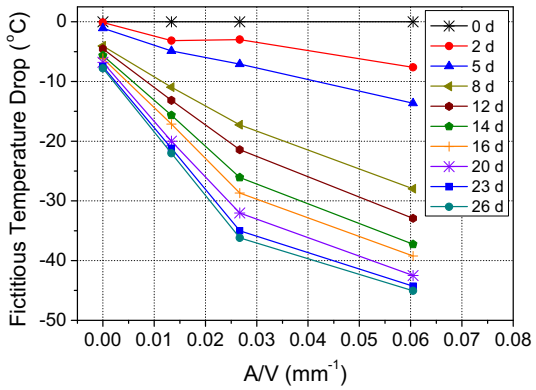

Fig. 6. Derived fictitious temperature drop vs. A/V ratio for thin concrete rings.

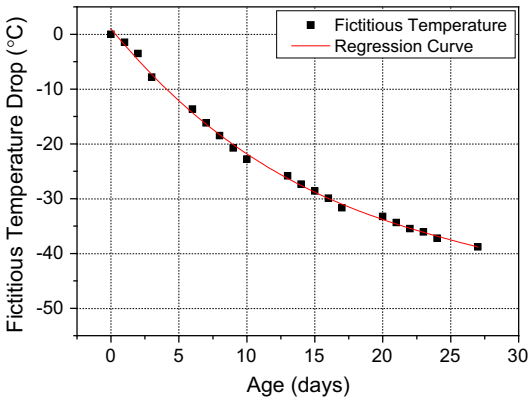

Fig. 8. Derived fictitious temperature drop vs. age for a thin elliptical ring ($a \times b = 150 \times 60$ mm^2).

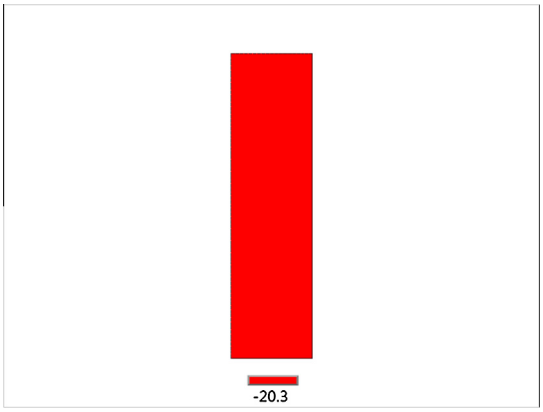

Fig. 7. Fictitious temperature field with temperature drops (in °C) in the concrete prism with $A/V = 0.027$ at the age of 10 days.

illustrates the derived temperature field for the concrete prism with two side surfaces exposed for drying ($A/V = 0.027$) at the age of 10 days, corresponding to the experimental longitudinal length change with a drying shrinkage strain of −203 με. Based on this analysis result, a uniform temperature drop of 20.30 °C would be applied on a concrete element, such as a thin concrete ring, with $A/V = 0.027$ causing the same mechanical effects as shrinkage does on the concrete element.

The corresponding A/V ratios of the circular and elliptical thin ring specimens were calculated based on their geometry and sealed condition. For a given concrete ring specimen with certain A/V ratio, the relationship between fictitious temperature drop and concrete age can be derived by the linear interpolation from the relationship between A/V and concrete age obtained from free shrinkage test of concrete prisms (i.e. Fig. 6) subjected to the same drying environment. Fig. 8, as the outcome of this analysis, showed the fictitious temperature drop for the elliptical ring with $a \times b = 150 \times 60$ mm^2 and $A/V = 0.027$. A regression analysis was conducted to obtain continuous functions that can represent the age-dependent uniform fictitious temperature drop applied to the thin ring specimen with the same effects as shrinkage does.

3.1.2. Thick ring specimens

With the increase of the thickness of a concrete element, the influence of moisture gradient across the thickness becomes more and more significant and cannot be neglected. It is therefore believed that the assumption of a uniform moisture loss, consequently uniform shrinkage, therefore uniform fictitious temperature field, across the thickness of the ring wall adopted for analysing thin rings is not appropriate for thick rings [4]. The temperature distribution across a thick ring wall should correspond to the moisture distribution in a 75 mm-thick concrete wall with only one side surface exposed for drying. According to the experimental investigation conducted by Weiss [20], the humidity in a normal strength concrete specimen at any age and position can be calculated by the following equation:

$$H(x,t) = H_{INTERNAL} - (H_{INTERNAL} - H_{EXPOSED})(10^{-(A_1 D + A_2) t^{(B_2 + B_1 \ln(D))} \frac{x}{D}}) \quad (1)$$

where $H(x,t)$ is the relative humidity at the depth x from the drying surface, $H_{INTERNSL}$ is the internal humidity of concrete if the specimen is completely sealed (in this paper $H_{INTERNAL}$ was assumed to be 100%), $H_{EXPOSED}$ is the relative humidity at the exposed surface of the specimen. According to Bažant and Najjar [23], the relative humidity of an exposed concrete surface can be evaluated by assuming an additional thickness on top of an exposed concrete surface, i.e. the equivalent surface thickness, between ambient environment and the physically exposed concrete surface. In this study, the ambient environmental humidity was 50%. Comparing analytical results with experimental ones, Bažant and Najjar [23] reported that the value of the equivalent surface thickness is 0.75 mm. Meanwhile, the coefficients A_1, A_2, B_1, and B_2 in Eq. (1) were determined as 0.2007, −1.0455, 0.0865 and −0.9115, respectively, for normal strength concrete by Weiss [20]. D is the overall depth of a concrete specimen, which was 75 mm in this study. In line with these, the humidity distribution within a concrete specimen can be determined using Eq. (1). Fig. 9 presents an example of relative humidity profiles, calculated based on Eq. (1), across the wall of a thick concrete ring at various ages when subject to outer circumferential drying. It can be seen from Fig. 9 that due to this additional surface layer, the relative humidity at the exposed concrete ring surface, i.e. the outer circumferential surface, is slightly higher than the ambient humidity of 50%. The humidity in a concrete ring increases across the ring wall thickness from the outer circumferential surface to the inner circumferential surface that is considered to be sealed as it contacts the central restraining steel ring. It can be seen from Fig. 9 that the humidity inside the concrete near the inner circumferential surface almost reaches 100%. Overall humidity in a concrete ring decreases as age increases which is reasonable as more water has been consumed by cement hydration as concrete gets mature.

Since the volumetric change of concrete can be divided into shrinkage caused by cement hydration (i.e., autogenous shrinkage) and that caused by moisture movement (drying shrinkage), two fictitious temperature drops, which reflect these two factors respectively, can be derived using the results of the free shrinkage test. For the concrete prism with all surfaces sealed in free

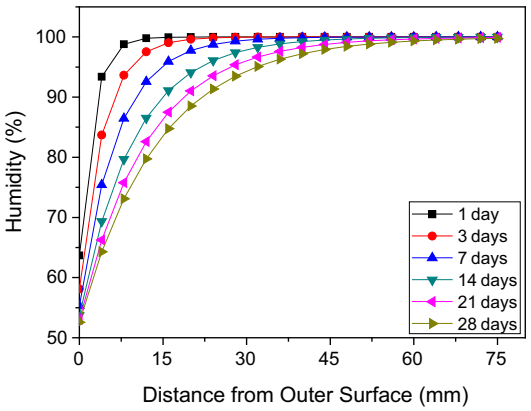

Fig. 9. Humidity distribution across the wall of a thick concrete ring at various ages when subject to outer circumferential drying.

shrinkage test, there is no moisture loss caused by environmental drying so the volume change of the prism can be regarded as purely resulting from cement hydration, i.e. autogenous shrinkage. Therefore, a uniform fictitious temperature drop can be obtained by measuring the shrinkage of all surfaces-sealed concrete prisms. On the other hand, the volumetric change caused by drying shrinkage can be derived from the difference of shrinkage in prisms between those with all side surfaces sealed and those with one side surface exposed. On the other hand, according to Moon et al. [6], the relationship between concrete shrinkage and relative humidity within a concrete element can be assumed as linear [6]. Since the humidity distribution in a concrete element at various ages has been determined by Eq. (1), the fictitious temperature drop acting on the exposed surface of a concrete specimen at any particular age can be derived according to the volumetric change caused by environmental drying. As an example, Fig. 10 illustrates the fictitious temperature field for the concrete prism with one side surface exposed to drying at the age of 10 days, corresponding to the scenario of experimental longitudinal length change with the shrinkage strain of -81 με. Based on this analysis result, a non-uniform temperature field with different temperature drops (see Fig. 10) would be applied to a thick concrete ring across its wall that causes the same mechanical effects as shrinkage does on the thick concrete ring.

As an outcome of such analysis, Fig. 11 presents the fictitious temperature drop at the exposed surface of a thick concrete ring with respect to age. In the combined thermal–structural analysis, the derived age-dependent fictitious temperature fields can be used to simulate the mechanical effects as shrinkage does.

3.2. Cracking age

In numerical analyses, the fictitious temperature fields derived in Section 3.1 were applied on a ring specimen to represent shrinkage effect. Once the shrinkage caused by the fictitious temperature fields is restrained by the inner steel ring, tensile stress will be developed in the concrete ring surrounding it. In this study, a maximum circumferential tensile stress cracking criterion was adopted for determining crack initiation in thin concrete rings. When the maximum circumferential tensile stress caused by the fictitious temperature field exceeds the tensile strength of concrete, cracks will initiate. While in a thick concrete ring, there is an obvious moisture gradient across the concrete ring wall, in which the shrinkage strain is much higher on the exposed surface than within concrete. Consequently, the circumferential tensile stress along the exposed concrete ring surface will be much higher than that within the ring body and cracking will initiate on the exposed surface. It has been found by Weiss [10] that the circumferential tensile stress will reach as high as 7 MPa at 7 days, which obviously exceeds the tensile strength of normal strength concrete and physically, is impossible. On the other hand, it has been found from this study no thick concrete ring cracked earlier than 18 days (see Table 1). Therefore, it can be reasonably concluded that maximal tensile stress-based cracking criterion underestimates crack resistance of concrete in thick rings and does not apply to thick concrete rings. Therefore, a fracture mechanics-based method is used to predict the cracking age in the thick concrete ring specimens. The details will be presented in the following sections.

3.2.1. Strength, modulus of elasticity and initial fracture toughness of concrete

Mechanical properties, in this case splitting tensile strength f_t and elastic modulus E_c, of concrete at 1, 7, 14 and 28 days were physically measured using 100 mm-diameter and 200 mm-length cylindrical specimens cured in the environment as the concrete ring specimens i.e. 23 °C and 50% RH, . Regression analyses were conducted on experimental data to obtain continuous equations that can represent the age-dependent mechanical properties of concrete. It was found that elastic modulus, E_c in GPa, of the concrete at early ages can be predicted using Eq. (2):

$$E_c(t) = 0.0002t^3 - 0.0134t^2 + 0.3693t + 12.715 \quad (t \leqslant 28) \tag{2}$$

and its splitting tensile strength, f_t in MPa, can be obtained using Eq. (3):

$$f_t(t) = 1.82t^{0.13} \quad (t \leqslant 28) \tag{3}$$

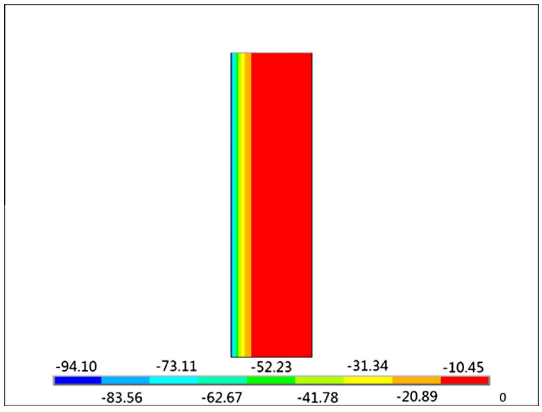

Fig. 10. Fictitious temperature field with temperature drops (in °C) in the concrete prism with one side surface exposed for drying at the age of 10 days.

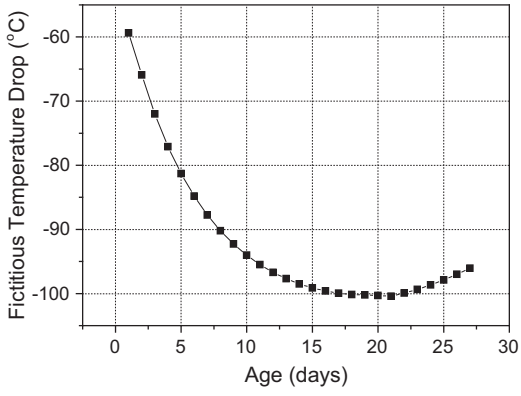

Fig. 11. Derived fictitious temperature drop at the exposed surface of a thick concrete ring with respect to concrete age.

In both equations, t is the age (in days) of concrete. The values of E_c and f_t for concrete at other ages that were not directly measured can be obtained from Eqs. (2) and (3), respectively.

Also, notched concrete beams were tested under three-point bending to measure the initial fracture toughness, K_{IC}^{ini}, of concrete at 1, 3, 7, 14 and 28 days. All notched beams have a cross-section of $100 \times 100\ mm^2$ and a length of 500 mm with the test span of 400 mm. The notch was set at the middle span of the beam with the initial depth of 33 mm, i.e., 1/3 of the overall depth of beam section. Details of the measurement method towards the initial fracture toughness, K_{IC}^{ini}, of concrete can be referred to Reference [24]. The notched beams for the fracture test were cured in the 23 °C and 50% RH environment, same as for concrete rings and cylinders. Based on the results of regression analyse, the initial fracture toughness, K_{IC}^{ini} of the concrete at early ages can be predicted using Equation (4):

$$K_{IC}^{ini} = 0.0011t^3 - 0.0574t^2 + 1.016t + 10.04 \quad (t < 14)$$
$$= -0.002t^2 + 0.1429t + 14.3 \quad (14 \leqslant t \leqslant 28) \tag{4}$$

As it is well known, early-age stress relaxation occurs as a result of concrete creep. Therefore, it is necessary to estimate the magnitude of creep when simulating the stress development in a concrete ring. Characterising creep of concrete is challenging as it depends on the stress level, specimen age, loading age, degree of hydration, temperature and drying condition. In this study, the age-dependent effective elastic modulus of concrete adopted in numerical analyses was taken as 60% of the value obtained from Eq. (2) to account for creep effects. A similar measure in reducing elastic modulus to take into account creep effect was also taken by Moon et al. [6] when analysing cracking in circular concrete rings under restrained shrinkage.

3.2.2. Numerical analysis

Numerical analyses were carried out on a series of ring specimens with various geometries, circular and elliptical, to study stress development, crack initiation and propagation in concrete rings subject to restrained shrinkage. The concrete ring specimens investigated in this study all had a depth of 75 mm with the inner steel ring having a wall thickness of 12.5 mm. To investigate the effects of concrete wall thickness on cracking, two wall thicknesses, i.e., 37.5 and 75 mm, were examined. Accordingly, in numerical analyses, contact element with zero friction between the contact pair was utilised to simulate this measure in conducting concrete ring tests. In numerical analyses, concrete shrinkage effect was simulated by fictitious temperature fields applying on ring specimens. For thin rings with a 37.5 mm-thick wall, a uniform temperature field with zero gradient across concrete ring wall was adopted, which is derived in Section 3.1.1. For thick ring specimens with a 75 mm-thick wall, considering the effect of moisture gradient across the wall, different fictitious temperature drops were applied across the ring wall. The temperature fields are derived using the approach described in Section 3.1.2. Inputting these parameters into finite element analysis, the time-dependent circumferential stress/stress intensity factor in concrete rings can be obtained.

In case of thick rings, a fracture mechanics-based cracking criterion was adopted for determining cracking age. For this purpose, a pre-crack with 2 mm long is set on the outer circumference of a thick elliptical ring along its minor axis. The maximum circumferential tensile stress occurring at this region with respect to the elastic analysis results is elaborated later. To consider the softening behaviour in micro-cracks, the fictitious crack model [25] is introduced in the fracture analysis through establishing softening stress (σ)–crack opening displacement (w) relationship of concrete. In this paper, the bilinear expression for σ–w (see Fig. 12) is chosen in the proposed numerical approach that is presented as follows:

$$\sigma = f_t - (f_t - \sigma_s)\frac{w}{w_s}, \quad 0 \leq w \leq w_s \tag{5}$$

$$\sigma = \sigma_s \frac{w_0 - w}{w_0 - w_s}, \quad w_s \leq w \leq w_0 \tag{6}$$

$$\sigma = 0, \quad w \geq w_0 \tag{7}$$

According to Peterson [26], σ_s, w_s and w_0 can be determined as follows:

$$\sigma_s = f_t/3 \tag{8}$$

$$w_s = 0.8G_F/f_t \tag{9}$$

$$w_0 = 3.6G_F/f_t \tag{10}$$

where w_0 is the displacement of the terminal point on the σ–w curve beyond which no stress can be transferred, i.e. the stress-free crack width, w_s and σ_s is the displacement and stress, respectively, corresponding to the break point in the bilinear σ–w relationship (see Fig. 12). These parameters and the σ–w relationship can be derived given the fracture energy G_F and the tensile strength f_t. Here, f_t is obtained from Eq. (3) and G_F is from the formula recommended by CEB-FIP model code 2010. A concrete crack propagation criterion based on initial fracture toughness has been established and validated in Reference [24], which is found to be able to predict the whole fracture process of concrete [27]. In this study, this criterion is introduced to analyse crack initiation and propagation in concrete rings subject to the restrained shrinkage, and singular elements are used to calculate stress intensity factor (SIF) at the crack tip. This criterion can be described as following: a crack begins to propagate when the difference, between the stress intensity factors K_I^S caused by the applied load (i.e., shrinkage effect in case of concrete rings) and K_I^σ by the cohesive stress, exceeds concrete's initial fracture toughness K_{IC}^{ini}. The crack propagation criterion can be described as follows:

$$K_I^S - K_I^\sigma < K_{IC}^{ini}, \text{ crack does not propagate} \tag{11}$$

$$K_I^S - K_I^\sigma = K_{IC}^{ini}, \text{ crack is in the critical state} \tag{12}$$

$$K_I^S - K_I^\sigma > K_{IC}^{ini}, \text{ crack propagates} \tag{13}$$

Since the fictitious temperature fields, which can represent the nonlinear distribution of moisture across a concrete ring wall, were derived in Section 3.1.2, K_I^S at the tip of the pre-crack can be calculated by applying the fictitious temperature fields on the concrete

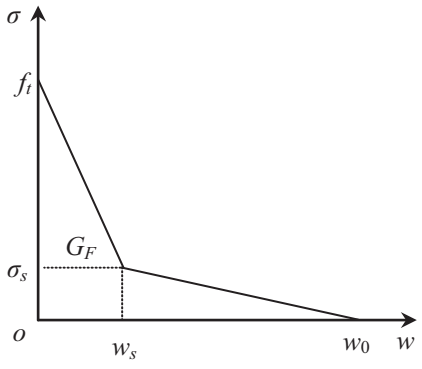

Fig. 12. Bilinear σ–w softening curve for concrete.

ring. K_I^{σ} is calculated based on the cohesive stress acting on a micro-crack, in which the cohesive stress is determined through Eqs. (5)–(7). At any specific age, crack propagation status can be determined by comparing $K_I^S - K_I^{\sigma}$ and K_{IC}^{ini}. It can be seen that at early ages, the shrinkage effect of concrete is not strong enough to drive crack propagation. With the increase in age, the shrinkage effect of concrete enhances. Once Eq. (12) is satisfied, a crack starts to propagate. After that, a crack length increment $\Delta a = 2$ mm is enforced and the iterative process is carried out again until a crack propagates throughout the whole ring wall. The details of the iterative process for predicting crack propagation based on the crack propagation criterion described in Eqs. (11)–(13) can be referred to Reference [24].

4. Results and discussion

4.1. Crack position

For a ring test, it is desirable if the position of cracking can be predicted in advance so that the resources required for detecting crack initiation and tracking crack propagation can be minimised during the experiment. For circular rings, it is impossible to predict the position of initial cracking due to the equal opportunity of cracking along their circumference. However, due to the geometrical effect of an elliptical ring, stress concentrations may develop at a specified position close to the vertices on the major/minor axis of the elliptical circumference as per elastic analysis. Experimental results of some thin rings support this assumption (see Fig. 13(a) and (b)). According to experimental results, for elliptical rings with $a \times b = 150 \times 60$ mm^2 (see Fig. 13(a)) and $a \times b = 150 \times 75$ mm^2 (see Fig. 13(b)), cracks initiated close to the vertices on the major axis of the inner elliptical circumference; for rings with $a \times b = 150 \times 125$ mm^2 (see Fig. 13(c)), crack occurred close to the minor axis. It can be seen from the circumferential stress contour (see Fig. 14(a) and (b)) that the stress concentration is significant in elliptical concrete rings with $a \times b = 150 \times 60$ mm^2 and 150×75 mm^2. The stress in the two vertices on the major axis of the inner elliptical circumference is much greater than that in any other zone. On the other hand, according to the circumferential stress contour shown in Fig. 14(c), the variation of tensile stress along the circumferential direction is not sharp and the stress concentration is not significant either. Similar to circular rings, the actual crack position observed from experiment may be mainly depended on defects of concrete, which results in the actual crack position different from the predicted along the ring circumference. Fig. 15 presents crack positions in three thick ring specimens observed from experimental work. It can be seen that, different from the scenario observed of thin ring specimens, some cracks (see Fig. 15) occurring between the major and minor axes were not in the vertices on the major or minor axis of the outer elliptical circumference. This cracking position can be explained based on numerical results as following. According to the circumferential stress contour (see Fig. 16) obtained from numerical analysis of a thick ring, the variation of circumferential stress along the radial direction is not sharp and stress concentration is not significant either. The thick elliptical geometry cannot provide a higher degree of restraint to concrete surrounding it and thus enhance the circumferential tensile stress developed in thick rings as it does in thin ones.

4.2. Cracking age and evolution of stress/SIF

To verify the numerical model developed in this study, a series of circular and elliptical ring specimens with various geometries subject to restrained shrinkage were analysed. Fig. 17 presents the maximum circumferential tensile stress developed in various thin rings obtained from numerical analyses. The maximum circumferential tensile stress was chosen from the mid-height section of a concrete ring specimen as per Hossain and Weiss [3]. When the maximum circumferential tensile stress developed in a concrete ring reaches the tensile strength of concrete, a crack initiates and the age at the interaction point gives the cracking age (see Fig. 17).

Fig. 18 presents the evolution of SIF caused by the shrinkage effect and cohesive stress with respect to age in a series of thick concrete rings. A crack will propagate when SIF caused by the combined effects of shrinkage and cohesive force exceeds initial

(a) $a \times b$=150×60 mm^2 (b) $a \times b$=150×75 mm^2 (c) $a \times b$=150×125 mm^2

Fig. 13. Cracks in various thin ring specimens observed from experiment.

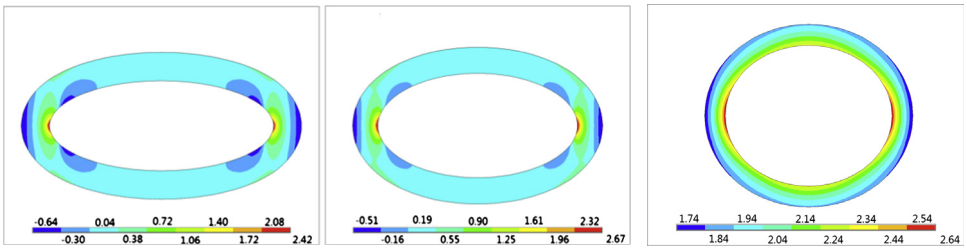

(a) $a \times b$=150×60 mm^2 (12 days) (b) $a \times b$=150×75 mm^2 (11 days) (c) $a \times b$=150×125 mm^2 (20 days)

Fig. 14. Circumferential stress contour in thin ring specimens at the age of crack initiation.

Please cite this article in press as: Dong W et al. Effects of specimen size on assessment of shrinkage cracking of concrete via elliptical rings: Thin vs. thick. Comput Struct (2016), http://dx.doi.org/10.1016/j.compstruc.2015.12.005

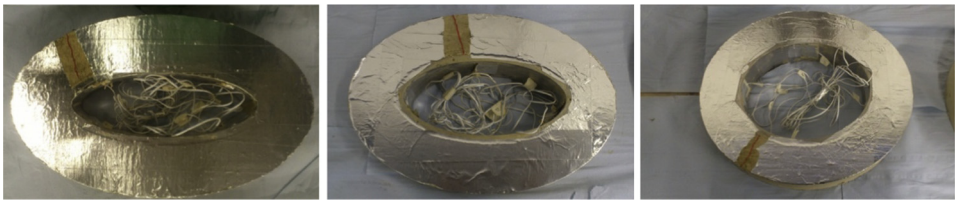

(a) $a\times b$=150×60 mm^2 (b) $a\times b$=150×75 mm^2 (c) $a\times b$=150×125 mm^2

Fig. 15. Crack in thick ring specimens observed from experiment.

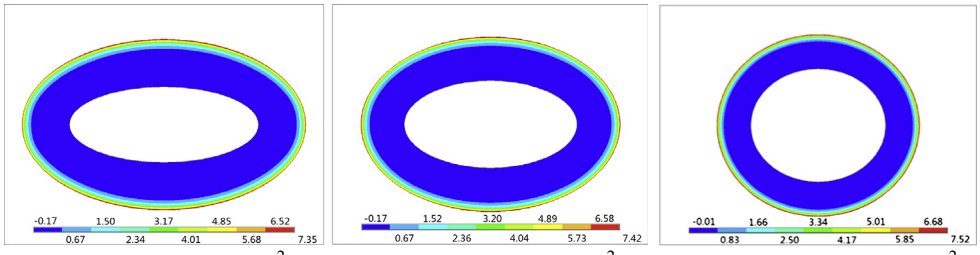

(a) $a\times b$=150×60 mm^2 (b) $a\times b$=150×75 mm^2 (c) $a\times b$=150×125 mm^2

Fig. 16. Circumferential stress contour in thick ring specimens at the age of 7 days.

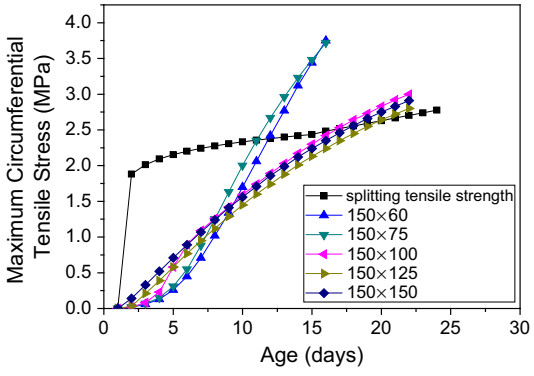

Fig. 17. Maximal circumferential tensile stress in thin rings with respect to age from numerical analysis.

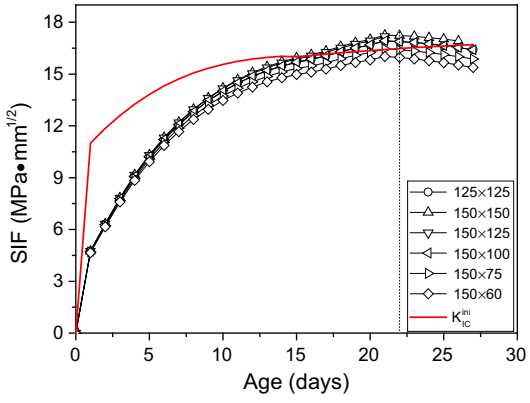

Fig. 18. SIF in thick concrete rings with respect to age.

fracture toughness, i.e. Eq. (13) is satisfied, with the corresponding age denoted as t_n. It indicates a new micro-crack will form, and the cohesive stress will be re-distributed along the fracture process zone at time t_n. Then, SIF caused by shrinkage and cohesive stress is recalculated by giving a 2 mm increment in crack length and compared with the initial fracture toughness at time t_n again. If Eq. (11) is satisfied, i.e. $K_I^S - K_I^\sigma < K_{IC}^{ini}$, the crack will not propagate. The numerical procedure moves to next age, say time t_j, with all materials parameters and applied load (in this case fictitious temperature fields) replaced by their corresponding values at age t_j. Comparison between SIF and initial fracture toughness will be repeated until Eq. (13) is satisfied. Once Eq. (13) is satisfied, a crack will propagate again with a length increment in this case 2 mm.

Fig. 19 presents the evolution of SIF with respect to crack length for various thick rings at their cracking age (with crack age in days shown in the brackets). It can be seen that the values of $K_I^S - K_I^\sigma$ at cracking age are greater than K_{IC}^{ini} at the concrete age of 28 days. It indicates that the crack length will keep increasing after a crack starts propagation at the first step. This is to say, once a crack begins to propagate, it will keep propagating across the whole ring wall for a restrained thick concrete ring. The cracking ages obtained from numerical analyses and experiment are listed in Table 1 for a series of circular and elliptical, thin and thick ring specimens. It can be reasonably concluded from experimental results that ring geometry has a significant effect on cracking sensitivity of thin ring specimens subject to restrained shrinkage. For thin rings, cracking age depends on the degree of stress concentration in a concrete ring, which further depends on the geometry factor a/b of an elliptical ring. When a/b is between 2 and 3, an elliptical ring can provide a higher degree of stress concentration to concrete surrounding it. At the same time, it is acknowledged that, with the increase of concrete wall thickness, the influence of elliptical geometry on crack sensitivity decreases. In fact, when concrete wall thickness increases from 37.5 to 75 mm, the stiffness of the concrete ring increases while the stiffness of the central restraining steel ring does not change. Therefore, the restraint effect provided by the inner steel ring becomes relatively weaker resulting in thick rings cracking later than thin ones. Also, according to numerical and experimental results, the failure mechanism in thin and thick concrete rings exhibits significantly different features. In thin rings, the crack initiation is a result of the restraining effect from the central steel ring. But things are different in thick rings. Due to the nonlinear distribution of humidity, therefore,

Please cite this article in press as: Dong W et al. Effects of specimen size on assessment of shrinkage cracking of concrete via elliptical rings: Thin vs. thick. Comput Struct (2016), http://dx.doi.org/10.1016/j.compstruc.2015.12.005

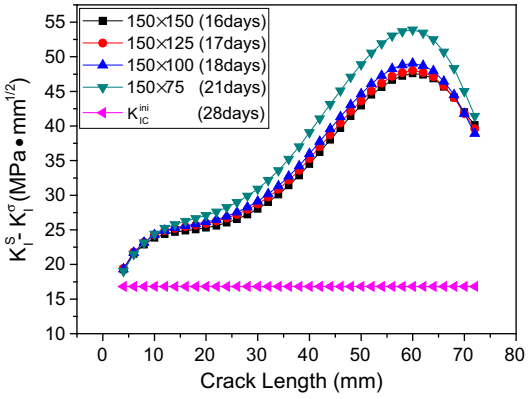

Fig. 19. Evolution of SIF with crack propagation in thick rings.

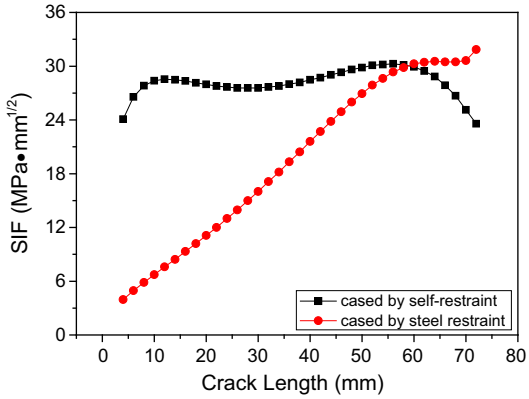

Fig. 20. Evolution of SIFs caused by various restraining effects with crack propagation in the 150 × 125 mm^2 thick ring.

the nonlinear distribution of shrinkage across the ring wall, the stress gradient is obvious across the wall of a thick ring. Tensile stress can be generated along the circumferential direction on the exposed surface of a concrete ring, even if there is no restraint provided by the central steel ring, i.e. no central steel ring exists. Therefore, it is necessary to distinguish the effects from the self-restraint caused by nonlinear humidity distribution across a thick concrete ring wall and external restraint provided by the central steel ring. According to Hossain and Weiss [7], the circumferential tensile stress in concrete in a restrained ring specimen subjected to drying shrinkage consists of two parts: (1) the circumferential tensile stress caused by self-restraint in a concrete wall and (2) the circumferential tensile stress caused by the central steel ring restraining the shrinkage of concrete in the radial direction. In the numerical analyses of thick rings, the first part of the circumferential tensile stress can be calculated through analysing a concrete ring with non-uniform free shrinkage, due to nonlinear humidity distribution across the ring wall and without any external restraint. Rather the restraint comes from self-restraint, i.e. the restraint to a concrete element in a thick ring comes from surrounding concrete elements which exhibit different deformation (i.e., shrinkage). This self-restraint effect is enlarged in case of a closed shape such as the ring shape specimen in this study. The second part of the circumferential tensile stress caused by the central steel ring, can be calculated by applying a restraining pressure on the inner circumferential surface of a concrete ring [16]. Thus, the SIF caused by drying shrinkage (i.e. self-restraint along circumferential direction) and restraint shrinkage (i.e. external restraint along radial direction by the steel ring) can be obtained using finite element analyses.

As an example of such analysis, Fig. 20 presents the evolution of SIF with respect to crack propagation in a circular concrete ring with $a \times b = 150 \times 125$ mm^2. It can be seen from Fig. 20 that the SIF caused by self-restraint effect keeps almost constant with respect to crack length, i.e. remains almost unchanged when the distance between crack tip and the outer circumferential surface of the steel ring is greater than 15 mm. With the decrease in this distance (i.e. the crack tip getting closer to the outer circumferential surface of the steel ring), the effect of self-restraint which drives crack propagation is weakened. This can be explained by the high relative humidity which reaches nearly 100% (see Fig. 9), consequently lowering the shrinkage and crack propagation driving energy in the corresponding area (i.e. the area close to the inner circumferential surface). However, the SIF due to restraint from the central steel ring keeps increasing with the increase of crack length, i.e. with the crack tip getting closer to the outer circumferential surface of the steel ring. From Fig. 20, it can be concluded that in general crack propagation near the exposed outer circumferential surface of a thick concrete ring is mainly due to self-restraint caused by non-uniform circumferential drying, while crack propagation near the sealed inner surface, which contacts the steel ring, results from the combined effects of self-restraint and the external restraint from the central steel ring.

Meanwhile, according to the observation of acoustic emission conducted by Hossain and Weiss [7], crack initiation in a restrained concrete ring and the sudden strain drop recorded from the central restraining steel ring, considered as an indication of cracking, occurs at approximately the same time. Based on the numerical and experimental results, a crack will propagate throughout a concrete ring wall very quickly after it starts to propagate. This indicates that cracking of a thick concrete ring drying from its outer circumferential surface is mainly caused by the self-restraint due to a nonlinear moisture gradient rather than the external restraint from the central steel ring. Thus, it is necessary to point out here that, for 75 mm-thick concrete ring specimens with top and bottom surfaces sealed and the outer circumferential surface exposed to drying, the cracking age reports the crack resistance subject to non-uniform circumferential drying rather than restrained shrinkage as claimed by AASHTO PP34-99. These findings support experimental results that indicate that in case of thick rings, the elliptical central steel ring does not provide higher degree of restraint to surrounding thick concrete ring. Therefore, the thick elliptical concrete rings do not crack earlier than thick circular ones. If any sealing condition allows the moisture distribution, therefore shrinkage, across the ring wall become uniform, the self-restraint effect from the concrete itself will be largely reduced. In this case, the restraining effect applied to a thick concrete ring will mainly come from the central steel ring, i.e. external restraint, as desirable.

5. Conclusions remarks

A series of circular and elliptical, both thin and thick, concrete rings were tested under restrained shrinkage conditions until cracks initiated and propagated throughout the ring wall. The purpose of these tests was to investigate the effect of concrete ring geometry and wall thickness on the evolution of stress/stress intensity factor. By introducing fictitious temperature fields to represent the mechanical effect of shrinkage of concrete, a numerical model was developed for predicting stress/SIF evolution and cracking initiation/propagation in concrete rings subjected to restrained shrinkage. Different temperature fields were derived to take into account the effect of concrete wall thickness on moisture gradient, thus shrinkage strain, across a ring wall. Cracking age, position and stress/SIF evolution were predicted for a wide range of circular and elliptical concrete rings with various geometries under restrained

Please cite this article in press as: Dong W et al. Effects of specimen size on assessment of shrinkage cracking of concrete via elliptical rings: Thin vs. thick. Comput Struct (2016), http://dx.doi.org/10.1016/j.compstruc.2015.12.005

shrinkage. Numerical and experimental results were compared and it was found that they agreed reasonably well. The restraining mechanism in thick rings was discussed in depth based on numerical and experimental results, in which the self-restraint and external restraint effects were differentiated. Based on numerical and experimental results and discussion of the mechanism of the ring test, the following conclusions can be drawn:

(a) Cracking age of concrete rings under restrained shrinkage can be predicted by introducing appropriate fictitious temperature fields to simulate concrete shrinkage. For thin rings with a wall thickness of 37.5 mm as recommended by ASTM C1581/C1581M-09a, a uniform temperature field with zero gradient across the concrete ring wall is accurate enough for simulating the effect of shrinkage of concrete and age of crack initiation. For thick rings with a wall thickness of 75 mm as recommended by AASHTO PP34-99, fictitious temperature fields with a gradient consisting of different temperature drops across the concrete ring wall, is more appropriate for comparing cracking ages and characteristics of cracking evolution obtained from numerical analyses and experimental work.

(b) Thin and thick rings demonstrate different cracking behaviour when subject to restrained shrinkage. In thin rings, crack initiated from the inner circumferential surface and propagated towards the outer one. The restraining effect mainly comes from an external factor i.e., the central restraining steel ring. Therefore, an appropriate elliptical geometry can accelerate the cracking process as desirable for faster assessment of cracking potential of concrete or other cement-based materials. In thin elliptical rings, the maximum circumferential tensile stress occurred in the two vertices on the major axis of the inner elliptical circumference. Cracks initiated in these zones of rings having a geometrical factor a/b greater than 2 and propagated towards outer circumference. In thick elliptical rings, the maximum circumferential tensile stress occurred in the two vertices on the minor axis of the outer elliptical circumference resulting in that crack initiated in these zones and propagated towards the inner circumference. The restraint effect mainly comes from self-restraint from surrounding concrete due to non-uniform shrinkage caused by nonlinear moisture movement across a thick concrete ring wall. The external restraint effect from the central steel ring is relatively weak at the onset of crack propagation. A crack will propagate very quickly throughout thickness of a ring wall once it starts to propagate.

(c) Based on experimental results, the thin elliptical ring with a geometrical factor a/b between 2 and 3 is recommended to replace traditional circular rings for restrained shrinkage test. The elliptical ring can increase cracking sensibility and consequently shorten the test duration for faster and more reliable assessment of the cracking tendency of concrete and other cement-based materials. An increased wall thickness decreases the restraining effect provided by the inner steel ring on the surrounding concrete. This marks down the advantage of using thick elliptical ring specimens to replace circular ring specimens in shortening the restrained shrinkage ring test duration. Moreover, for thick ring specimens, crack initiation is due to the self-restraint of concrete caused by circumferential drying. Therefore, in order to assess cracking resistance of concrete subject to restraint, a thinner concrete wall should be selected in the ring test to enable uniform shrinkage strain across a concrete ring wall, minimising the self-restraint effect associated with the ring geometry. In the case of thick rings, if any sealing condition allows the moisture distribution, therefore shrinkage, across the ring wall become uniform, the self-restraint effect from the concrete itself will be largely reduced. In this case, the restraining effect applied to a thick concrete ring will mainly come from the central steel ring, i.e. external restraint. By such modification, the thick ring test recommended by AASHTO will better serve its purpose.

Acknowledgement

The financial support of the Engineering and Physical Sciences Research Council under the grant of EP/I031952/1, the National Natural Science Foundation of China under the grant of NSFC 51421064 and 51478083, and the fundamental research funds for the Central Universities under the grant of DUT14LK06 is gratefully acknowledged.

References

[1] ASTM. Annual book of ASTM standards. Concrete and aggregates; 2012.
[2] Shah SP, Weiss WJ, Yang W. Shrinkage cracking-can it be prevented? Concr Int 1998;20(4):51–5.
[3] Hossain AB, Weiss J. Assessing residual stress development and stress relaxation in restrained concrete ring specimens. Cement Concr Compos 2004;26(5):531–40.
[4] Moon JM, Weiss WJ. Estimating residual stress in the restrained ring test under circumferential dying. Cement Concr Compos 2006;28(5):486–96.
[5] Bentur A, Kovler K. Evaluation of early age cracking characteristics in cementitious systems. Mater Struct 2003;36(3):183–90.
[6] Moon JH, Pease B, Weiss J. Quantifying the influence of specimen geometry on the results of the restrained ring test. J ASTM Int 2006;3(8):1–14.
[7] Hossain AB, Weiss J. The role of specimen geometry and boundary conditions on stress development and cracking in the restrained ring test. Cem Concr Res 2006;36(1):189–99.
[8] Passuello A, Moriconi G, Shah SP. Cracking behavior of concrete with shrinkage reducing admixtures and PVA fibers. Cement Concr Compos 2009;31(10):699–704.
[9] Weiss WJ, Yang W, Shah SP. Influence of specimen size/geometry on shrinkage cracking of rings. ASCE J Eng Mech 2000;126(1):93–101.
[10] Weiss WJ, Shah SP. Restrained shrinkage cracking: the role of shrinkage reducing admixtures and specimen geometry. Mater Struct 2002;35(2):85–91.
[11] He Z, Zhou XM, Li ZJ. New experimental method for studying early-age cracking of cement-based materials. ACI Mater J 2004;101(1):50–6.
[12] He Z, Li ZJ. Influence of Alkali on restrained shrinkage behavior of cement-based materials. Cem Concr Res 2005;35(3):457–63.
[13] He Z, Li ZJ, Chen MZ, Liang WQ. Properties of shrinkage-reduced admixture-modified pastes and mortar. Mater Struct 2006;39(4):445–53.
[14] Ma BG, Wang XG, Liang WQ, Li XG, He Z. Study on early-age cracking of cement-based materials with superplasticizers. Constr Build Mater 2007;21(11):2017–222.
[15] Zhou XM, Dong W, Oladiran O. Assessment of restrained shrinkage cracking of concrete using elliptical ring specimens: experimental and numerical. ASCE J Mater Civil Eng 2014;26(12):871–8.
[16] Dong W, Zhou XM, Wu ZM. A fracture mechanics-based method for prediction of cracking of circular and elliptical concrete rings under restrained shrinkage. Eng Fract Mech 2014;131(12):687–701.
[17] Kovler K, Sikuler J, Bentur A. Restrained shrinkage tests of fiber reinforced concrete ring specimens: effect of core thermal expansion. ACI Mater J 1993;26(4):231–7.
[18] Shah HR, Weiss J. Quantifying shrinkage cracking in fiber reinforced concrete using the ring test. Mater Struct 2006;39(9):887–99.
[19] Shah SP, Ouyang C, Marikunte S, Yang W, Becq-Giraudon E. A method to predict shrinkage cracking of concrete. ACI Mater J 1998;95(4):339–46.
[20] Weiss WJ. Prediction of early-age shrinkage cracking in concrete [Ph.D. Dissertation]. Northwestern University; 1999.
[21] Hossain AB. Assessing residual stress development and stress relaxation in restrained concrete ring specimens [Ph.D Disseratation]. Purdue University; 2003.
[22] Zhou XM, Dong W, Oladiran OG, Wu ZM, Kastiukas G. Numerical and experimental assessment of the effects of specimen size on shrinkage cracking of concrete. In: Topping BHV, Iványi P, editors. Proceedings of the twelfth international conference on computational structures technology. Stirlingshire, UK: Civil-Comp Press; 2014. http://dx.doi.org/10.4203/ccp.106.239. Paper 239.
[23] Bažent ZP, Najjar LJ. Nonlinear water diffusion in nonsaturaturated concrete. Mater Struct 1972;25(5):3–20.

[24] Dong W, Wu ZM, Zhou XM. Calculating crack extension resistance of concrete based on a new crack propagation criterion. Constr Build Mater 2013;38(1):879–89.

[25] Hillerborg A, Modéer M, Petersson PE. Analysis of crack formation and crack growth in concrete by means of fracture mechanics and finite elements. Cem Concr Res 1976;6(6):773–81.

[26] Petersson PE. Crack growth and development of fracture zones in plain concrete and similar materials, Report No.TVBM-1006, Lund Institute of Technology, Sweden; 1981.

[27] Dong W, Zhou XM, Wu ZM. On fracture process zone and crack extension resistance of concrete based on initial fracture toughness. Constr Build Mater 2013;49(12):352–63.

Please cite this article in press as: Dong W et al. Effects of specimen size on assessment of shrinkage cracking of concrete via elliptical rings: Thin vs. thick. Comput Struct (2016), http://dx.doi.org/10.1016/j.compstruc.2015.12.005